PREPARATION OF VANADIUM PENTOXIDE NANOPARTICLE-DEPOSITED ALUMINA SUBMICRON PARTICLES FOR CATALYSTS WITHOUT SINTERING

PREPARATION OF VANADIUM PENTOXIDE NANOPARTICLE-DEPOSITED ALUMINA SUBMICRON PARTICLES FOR CATALYSTS WITHOUT SINTERING

Yoshiki Okada*, Yusuke Takahashi, Tomoki Minami and Takuya Kinoshita

Abstract

The formation of vanadium pentoxide (V_2O_5) nanoparticles immobilized on alumina (Al_2O_3) particles was studied in a methane/oxygen coflow diffusion-flame reactor. V_2O_5 nanoparticles formed by the decomposition of vanadium oxytriethoxide were deposited onto Al_2O_3 particles, which were introduced into the flame together with vanadium oxytriethoxide solution. To immobilize the V_2O_5 nanoparticles on Al_2O_3 particles, rapid cooling with a Laval nozzle was applied to the V_2O_5/Al_2O_3 particles formed in the flame. We found that it was possible to suppress the sintering of V_2O_5 nanoparticles on the Al_2O_3 particles when the Al_2O_3 particles were introduced into the flame at a temperature sufficiently high to soften the surfaces of the Al_2O_3 particles.

1 Introduction

V_2O_5 nanoparticles supported on metal oxide particles are used as catalysts for various reactions, including sulfur dioxide oxidation for sulfuric acid production[1)-3)]. However, the lifetime of V_2O_5 catalysts prepared by the usual liquid phase methods is not long, because their catalytic activities are gradually decreased during reactions due to sintering. Sintering of V_2O_5 catalyst nanoparticles is triggered by the fact that they migrate on the catalyst support, resulting in their aggregation and growth during reactions at high temperatures.

In our previous studies[4)], we successfully prepared silica (SiO_2) microsphere-supported nickel (Ni) nanoparticle catalysts that did not exhibit sintering. The method was based on the collision of Ni nanoparticles onto SiO_2 microspheres with surfaces softened by heating at sufficiently high temperatures, followed by rapid cooling of the Ni nanoparticle-deposited SiO_2 microspheres in our supersonic Laval nozzle. We observed some dents on the surfaces of SiO_2 microspheres, generated by the collision of Ni nanoparticles onto the soft SiO_2 microspheres. The rapid cooling of SiO_2 microspheres immediately after partial embedding of Ni nanoparticles into the dents of SiO_2 particles in the Laval nozzle was able to maintain the dents and immobilize Ni particles inside the dents. This immobilization prevented the sintering of Ni nanoparticles on the SiO_2 microspheres.

In the present work, our method for preventing the sintering of catalyst nanoparticles on

Department of Chemical, Energy and Environmental Engineering, Kansai University, Suita, Osaka 564-8680, Japan

∗ Correspondence to: Yoshiki Okada. E-mail: yokada@kansai-u.ac.jp

support particles was applied to the production of V_2O_5 nanoparticles supported on Al_2O_3 particles in our flame reactor. The flame conditions were investigated for realizing temperatures sufficiently high to soften the surfaces of Al_2O_3 particles, and to suppress the sintering of V_2O_5 nanoparticles.

2 Experimental Method

Figure 1 presents our experimental setup. The details of our flame reactor are available in our previous papers[5)-7)]. A coflow diffusion burner consisting of four concentric tubes was used. The droplets of the precursor solution emerged from the two-fluid nozzle inside the centermost tube of the burner. In this study, no gas flowed through the second tube of the burner, where generally a sheath gas is flowed to control the temperature and length of the flame. A mixture of 0.6 L/min – 1.6 L/min of CH_4 gas and 0.2 L/min of O_2 gas, and 4.0 L/min – 6.0 L/min of O_2 gas flowed through the third and fourth tubes of the burner, respectively. A cold quenching 12.5 L/min N_2 gas at approximately 203 K flowing through a methanol slush bath at 176 K blew on the tip of the flame from the eight nozzles of the gas ring.

The supersonic Laval nozzle, with a throat diameter of 2.0 mm, was positioned such that the inlet of the nozzle was approximately 5 mm downstream from the tip of the flame. The pressures in the upstream and downstream regions of the Laval nozzle were maintained at 103 kPa and 22 kPa, respectively. The adiabatic expansion in the supersonic Laval nozzle,
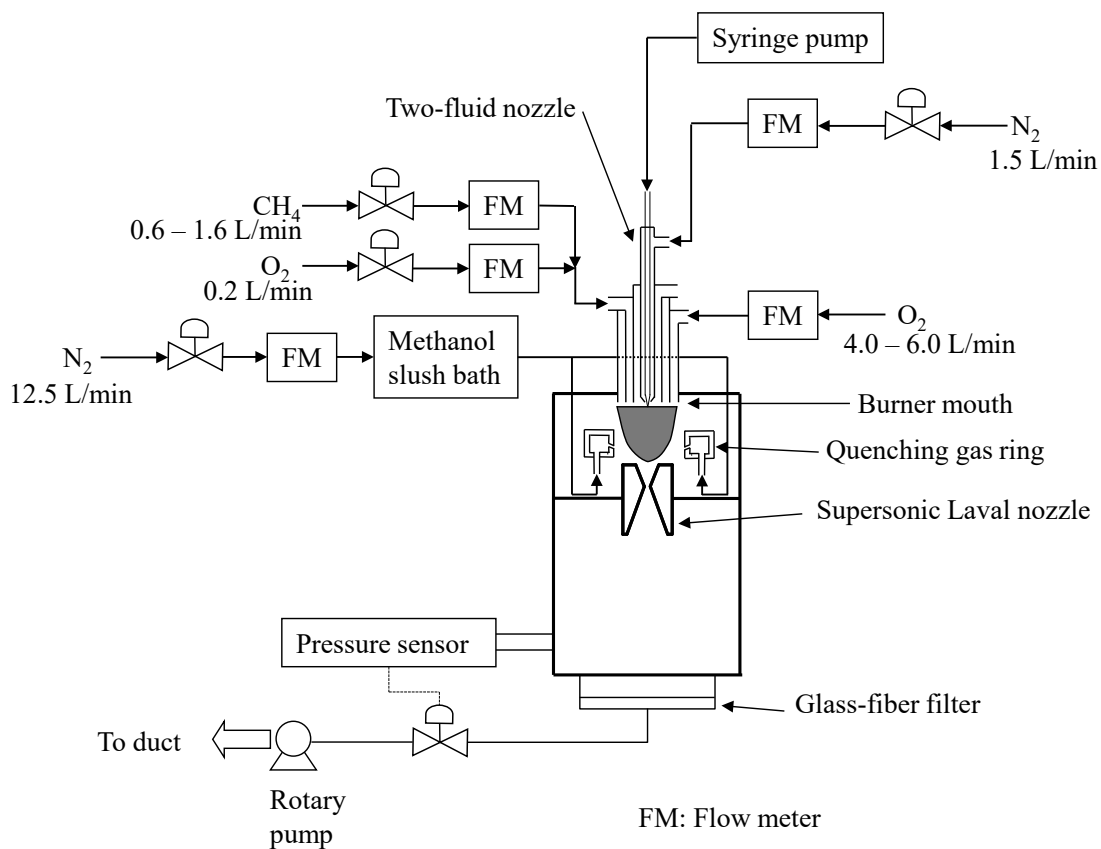

Fig. 1 Experimental setup.

PREPARATION OF VANADIUM PENTOXIDE NANOPARTICLE-DEPOSITED
ALUMINA SUBMICRON PARTICLES FOR CATALYSTS WITHOUT SINTERING

3

caused by large differences in pressure between the upstream and downstream of the nozzle, can rapidly lower the internal energy of the gas and the temperature of the produced particles passing through the nozzle.

The precursor solution was made by dissolving 0.05 mL of vanadium(V) oxytriethoxide (VOTE, $OV(OC_2H_5)_3$ 95%) into 80 mL of ethanol (CH_3CH_2OH 99.5%) and 20 mL of ethylene glycol ($HOCH_2CH_2OH$ 99.5%). A mixture of 1.0 g of spherical alumina particles (AO-502, Admatechs Co., Ltd.) with an average diameter of approximately 260 nm and the above-mentioned precursor solution was atomized through the two-fluid nozzle equipped with a syringe pump at a flow rate of 1.5 mL/min. The Al_2O_3 particles used were a mixture of γ-type, δ-type, and θ-type alumina with a specific surface area of approximately 6.5 m^2/g.

The produced particles were collected on a glass-fiber filter. The population of chemical elements of the produced particles was observed by energy dispersive X-ray (EDX) spectroscopy using a field emission-type scanning electron microscope (FESEM, S-4800, Hitachi High-Technologies Corp.). To obtain distributions of the diameter of V_2O_5 and Al_2O_3 particles, the diameters of approximately 200 or more particles produced under each condition were analyzed by FESEM. The change in V_2O_5 nanoparticle diameter on an alumina particle caused by the sintering of V_2O_5 nanoparticles was investigated using the FESEM images. X-ray diffraction (XRD) patterns of the produced particles were obtained with a diffractometer (RINT-TTRIII/RX, Rigaku Corp.) operating with Cu (Kα) radiation.

3 Results and Discussion

Figure 2 shows an XRD spectrum of the powder prepared from the precursor solution made by dissolving VOTE into ethanol and ethylene glycol without the Al_2O_3 particles when the flow rates of CH_4 gas through the third and O_2 gas through the fourth tubes of the burner were 0.6 L/min and 4.0 L/min, respectively. The XRD pattern of the synthesized powder was confirmed to be V_2O_5.
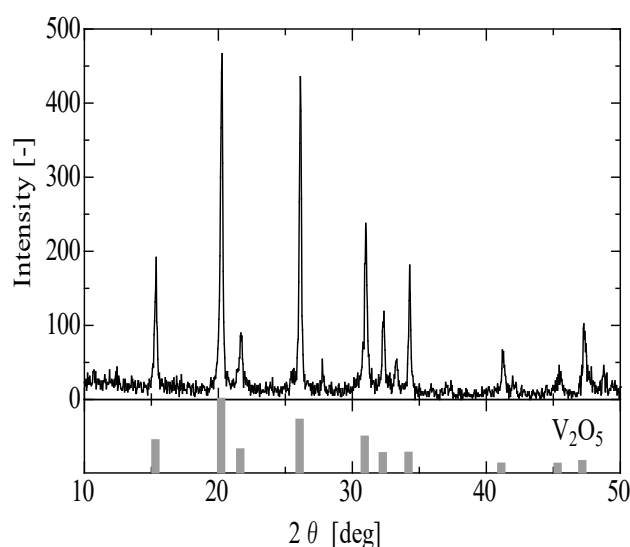

Fig. 2 XRD spectrum of particles produced, and XRD pattern of V_2O_5.

Figure 3(a) contains an FESEM image of the alumina particles used in this study. The particles had smooth surfaces and an average diameter of approximately 260 nm. Figure 3(b) shows an FESEM image of V_2O_5 nanoparticles deposited on Al_2O_3 particles under the same gas conditions as in Fig. 2. The highest temperature in the flame was measured at approximately 1,773 K using a thermocouple thermometer. Many V_2O_5 nanoparticles were observed on the surfaces of Al_2O_3 particles.

Figure 4 shows an EDX spectrum of the particle shown in Fig. 3(b). The peak of Au in the figure originates from the Au sputtering film, which was used to cover the sample to ensure electrical conductivity. The peak of C originates from the carbon tape used to immobilize the sample particles on the stage. We observed the peaks of V and Al, but no peaks of other metal atoms in the spectrum. From the population of chemical elements in the EDX spectrum, it was found that the amount of vanadium atoms was 1.8 wt% on the Al_2O_3 particles. The results shown in Figs. 2, 3, and 4 suggested that the deposition of V_2O_5 nanoparticles on Al_2O_3 particles could be attained by the flame reaction. It was also found that approximately 70% of vanadium atoms in the precursor solution atomized into the flame were
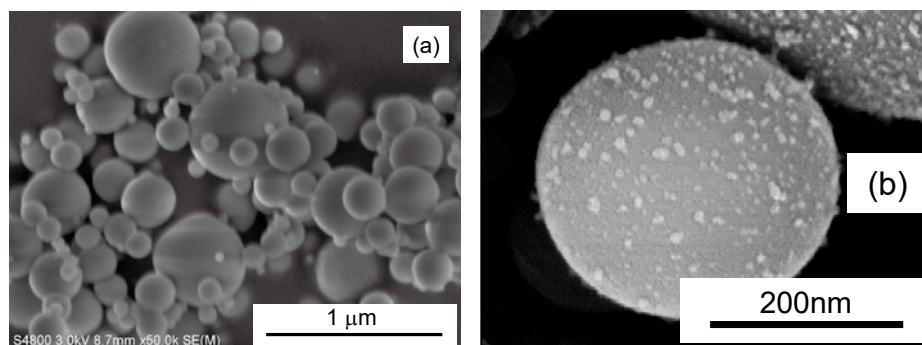

Fig. 3 FESEM images of (a) alumina particles used in this work; and (b) V_2O_5 nanoparticles deposited on alumina particles produced when the flow rates of CH_4 gas through the third and O_2 gas through the fourth tubes of the burner were 0.6 L/min and 4.0 L/min, respectively.

Fig. 4 EDX spectrum of a particle produced when the flow rates of CH_4 gas through the third and O_2 gas through the fourth tubes of the burner were 0.6 L/min and 4.0 L/min, respectively.
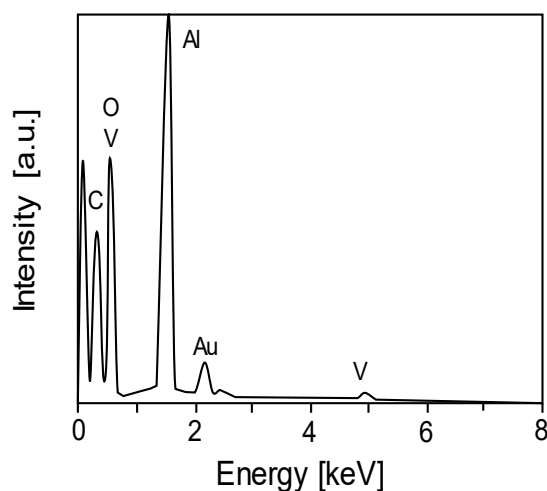
deposited on Al_2O_3 particles. It is probable that the rest of vanadium atoms were not supported on Al_2O_3 particles and were released as V_2O_5 nanoparticles through the filter to the outside of the reactor.

In order to investigate the sintering of V_2O_5 nanoparticles on alumina particles at high temperatures, we heated the as-synthesized particles shown in Fig. 3(b) at 673 K for 4 h in air. Figure 5 shows a FESEM image of V_2O_5 nanoparticles after the heat treatment (top), and the size distributions of V_2O_5 nanoparticles deposited on alumina particles before and after the heat treatment (bottom). The diameter of V_2O_5 nanoparticles increased after heating. This increase in diameter was recognized to be due to sintering during the heat treatment at 673 K for 4 h. The sintering of V_2O_5 nanoparticles could not be suppressed for V_2O_5/Al_2O_3 particles formed in the flame with the CH_4 gas flow rate of 0.6 L/min. We theorized that the surfaces of Al_2O_3 particles would become sufficiently soft by passing through the flame; however, we understood from the result exhibiting sintering that the surfaces were not soft enough to immobilize V_2O_5 nanoparticles on the surfaces.
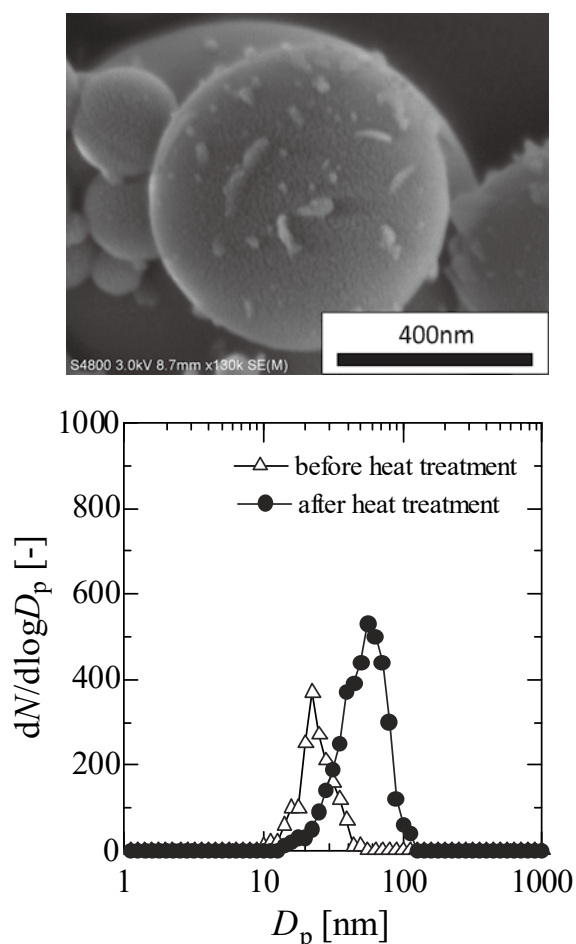

Fig. 5 FESEM image of V_2O_5 nanoparticles deposited on alumina particles shown in Fig. 3(b) after the heat treatment at 673 K for 4 h in the air (top), and the size distributions of V_2O_5 nanoparticles before and after the heat treatment (bottom).

Figure 6 shows the size distributions, before and after the heat treatment at 673 K for 4 h, of V_2O_5 nanoparticles on Al_2O_3 particles formed when we increased the CH_4 gas flow rate to realize a higher flame temperature. In this case, the flow rates of CH_4 gas through the third and O_2 gas through the fourth tubes of the burner were 1.0 L/min and 4.0 L/min, respectively. The highest temperature of this flame was approximately 2,073 K. In Fig. 6, there was an increase in the diameter of V_2O_5 nanoparticles after the heat treatment, although the increase was smaller than that in the case shown in Fig. 5. Again in this case, the sintering of V_2O_5 nanoparticles could not be suppressed. It was considered that the surface temperature of Al_2O_3 particles heated in the flame did not reach the range where the surfaces were sufficiently soft to hold tightly colliding V_2O_5 nanoparticles.

Figure 7 shows the size distributions of V_2O_5 nanoparticles on Al_2O_3 particles formed at a
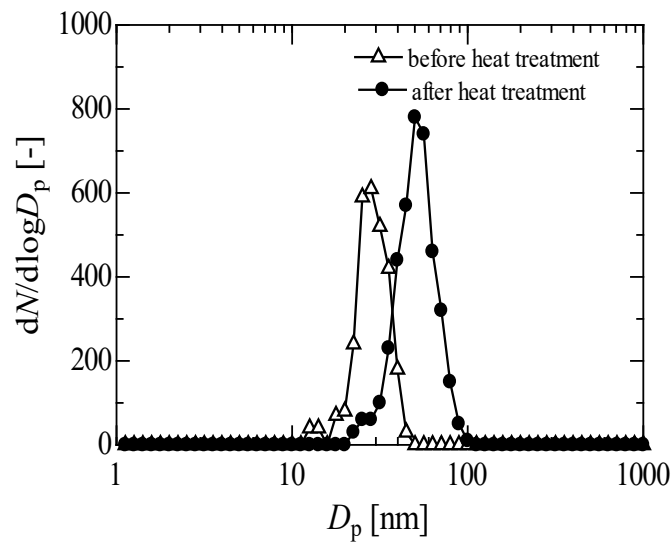

Fig. 6 Size distributions of V_2O_5 nanoparticles deposited on alumina particles formed when the flow rate of CH_4 gas was 1.0 L/min before and after heat treatment at 673 K for 4 h in air.

Fig. 7 Size distributions of V_2O_5 nanoparticles deposited on alumina particles formed when the flow rate of CH_4 gas was 1.6 L/min before and after heat treatment at 673 K for 4 h in air.
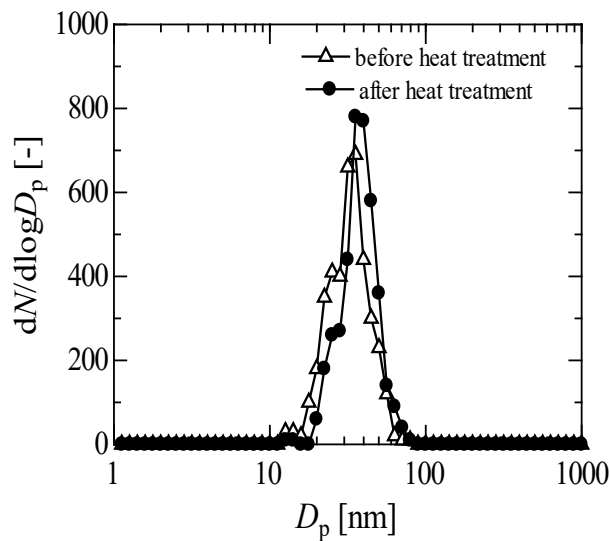
higher flow rate of CH_4 gas before and after the heat treatment at 673 K for 4 h. In this case, the flow rates of CH_4 gas through the third and O_2 gas through the fourth tubes of the burner were 1.6 L/min and 6.0 L/min, respectively. The highest temperature in this flame was over 2,273 K, too high to be measured by the thermocouple thermometer. The temperature of the gas at the inlet of the Laval nozzle was approximately 1,000 K. The population of vanadium atoms on Al_2O_3 particles was almost the same as that in the case shown in Fig. 3(b). Figure 7 indicates that the diameter of V_2O_5 nanoparticles after the heat treatment was almost the same as before the treatment. It was found that the sintering of V_2O_5 nanoparticles could be suppressed.

To explain the lack of sintering of V_2O_5 nanoparticles, the following is considered. Both V_2O_5 nanoparticles formed in the flame and Al_2O_3 particles passing through the flame entered the Laval nozzle immediately after exiting the flame. As the particles approached the 2.0 mm diameter throat 9 mm downstream from the inlet of the Laval nozzle, particle densities were increasing. The probability of collisions between V_2O_5 nanoparticles and Al_2O_3 particles likely increased, and many V_2O_5 nanoparticles were deposited onto Al_2O_3 particles in the region between the inlet and the throat of the Laval nozzle. If the surfaces of Al_2O_3 particles were sufficiently soft at these depositions, the V_2O_5 nanoparticles could sink into the soft Al_2O_3 particles due to the momentum of the colliding nanoparticles. The particles were then solidified and immobilized by the rapid cooling after passing through the throat of the Laval nozzle in the adiabatic expansion flow.

Figure 8 shows the size distributions of Al_2O_3 particles before and after passing through the flame in which the V_2O_5 nanoparticles shown in Fig. 7 were synthesized. No change was observed in the diameter of Al_2O_3 particles. It was found that the Al_2O_3 particles neither aggregated nor grew in the flame. The melting point of alumina is known to be 2,345 K. The highest temperature in the flame might have been higher than the melting point of alumina. However, aggregation and growth of Al_2O_3 particles due to melting of the surfaces was not observed because of the short residence time of Al_2O_3 particles in the flame. When the XRD
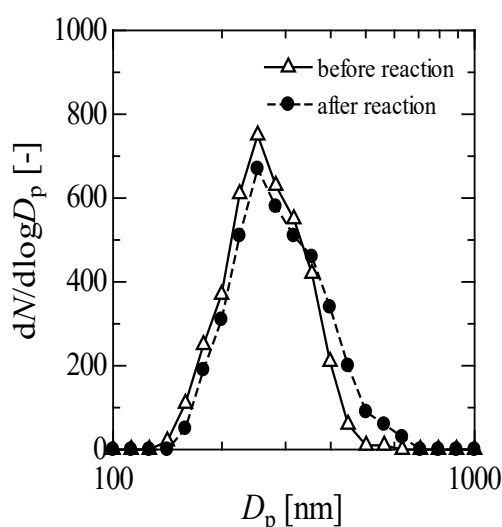

Fig. 8 Size distributions of Al_2O_3 particles before and after passing through the flame in which the V_2O_5 nanoparticles shown in Fig. 7 were synthesized.

spectra of Al_2O_3 particles before and after passing through the flame were compared, no change was observed in the XRD pattern. Consequently, it was also found that Al_2O_3 particles were thermally stable in the flame because of their short residence time. It was understood that the conditions of this flame were suitable from the viewpoint of temperature. The temperature of the flame was sufficiently high to soften the surfaces of Al_2O_3 particles enough to suppress sintering, but was below the range where the aggregation of Al_2O_3 particles and the phase transition of alumina occur.

4 Conclusions

We investigated the sintering of V_2O_5 nanoparticles deposited on Al_2O_3 particles formed in our flame reactor equipped with a rapid cooling system. It was found that the sintering of V_2O_5 nanoparticles could be suppressed by introducing Al_2O_3 particles into the flame at a high temperature, over 2,273 K, together with the precursor solution. The surfaces of Al_2O_3 particles softened in the flame at high temperature could immobilize V_2O_5 nanoparticles on the surfaces after rapid cooling in the supersonic Laval nozzle. We succeeded in forming V_2O_5 nanoparticles supported on Al_2O_3 particles that exhibited no sintering.

References

1) O.B. Lapina, B.S. Balʹzhinimaev, S. Boghosian, K.M. Eriksen and R. Fehrmann. Progress on the Mechanistic Understanding of SO_2 Oxidation Catalysts. *Catal. Today*, **51**, 469-479 (1999).

2) B.S. Balʹzhinimaev, N.P. Belyaeva, S.I. Reshetnikov, E.S. Yudina and A.A. Ivanov. Phase Transitions in a Bed of Vanadium Catalyst for Sulfuric Acid Production: Experiment and Modeling. *Chem. Eng. J.*, **84**, 31-41 (2001).

3) X. Wang, Y. Kang, D. Cui, J. Li and D. Li. Influence of Lanthanum Promoter on Vanadium Catalyst for Sulfur Dioxide Oxidation. *Catal. Commun.*, **118**, 39-45 (2019).

4) Y. Okada, S. Matsumoto, R. Sawai and T. Kinoshita. Formation of Non-Aggregated Nickel Nanoparticles for Catalysts by Gas-Phase Reaction. *J. Chem. Eng. Japan*, **50**, 511-515 (2017).

5) Y. Okada, H. Kawamura and H. Ozaki. Formation of Non-Agglomerated Titania Nanoparticles in a Flame Reactor. *J. Chem. Eng. Japan*, **44**, 7-13 (2011).

6) Y. Okada, A. Mizutori and D. Yamaoka. Formation of Non-Aggregated $Li_4Ti_5O_{12}$ Particles in a Flame Reactor. *Earozoru Kenkyu*, **32**, 52-57 (2017).

7) Y. Okada, T. Kubo and T. Kinoshita. Formation of TiO_2-SiO_2 Composite Oxide Particles in a Flame Reactor with a Rapid Particle-Cooling System. *Earozoru Kenkyu*, **34**, 5-10 (2019).